

BEYOND IEEE STD 115 & API 546: TEST PROCEDURES FOR HIGH-SPEED, MULTI-MEGAWATT PERMANENT-MAGNET SYNCHRONOUS MACHINES

Copyright Material IEEE
Paper No. PCIC-()

Daniel M. Saban, PE PhD[†]
Senior Member, IEEE
saban@ieee.org

Cassandra Bailey[†]
Member, IEEE & ASME
cbailey@directdrivesystems.net

Klaus Brun, PhD^{††}
kbrun@swri.org

Delvis Gonzalez-Lopez, PhD[†]
Member, IEEE
dgonzalez@directdrivesystems.net

[†] Direct Drive Systems 12880 Moore St., Cerritos, CA 90703 USA

^{††} Southwest Research Institute 6220 Culebra Road, P.O. Drawer 28510 San Antonio, Texas 78228-051 USA

Abstract - High-speed multi-megawatt permanent-magnet machines have been proposed in the literature and offered for sale in a variety of petro-chemical applications. Presently, the discussion of synchronous machines in both IEEE Std 115 [1] and American Petroleum Institute (API) 546 [2] exclude consideration of permanent-magnet synchronous machines. These machines pose special problems when attempting to apply the test procedures given for wound-field synchronous machines in that many of the tests rely on the ability to adjust the field strength. In addition, a permanent-magnet-rotor topology has different performance and robustness concerns than a wound-field machine that should be addressed. This paper attempts to outline a coherent method for evaluating high-speed permanent-magnet machines by extending the test procedures outlined in IEEE Std 115, and by presenting additional procedures specific to permanent-magnet machines. Extended application guidelines will be discussed for high-speed, multi-megawatt machines. The differences between the risk profile for permanent-magnet machines and wound-field machines will be highlighted with a particular emphasis on risk mitigation via test for the permanent-magnet machine.

Index Terms — Permanent magnet, high speed, synchronous, motor, generator

I. INTRODUCTION

Multi-megawatt high-speed PM machines are typified by robust rotor construction since they are typically speed-limited by the strength of the materials chosen. This narrows the rotor topology of choice to a surface-mount or embedded magnet construction with a retaining sleeve [3]. High pole-count machines may use a bracket or similar means to support the magnet [4], but this introduces additional complexity. In addition, either two- or four-pole machines are favored to minimize the operating frequency. A large magnetic gap is present to accommodate the not insignificant retaining sleeve; this tends to reduce the saliency of even embedded magnet designs such that they can be treated as or very close to a “round rotor” or non-salient design. The proposed methods described below are therefore focused on non-salient PM machines.

The rotor of a PM machine can be modeled using an equivalent field-current to represent the constant excitation (neglecting temperature effects) provided by the magnets [5]. The PM machine can then be thought of as the degenerate

case of a round-rotor wound-field synchronous machine (WFSM), but with no access to field control or rotor windings.

This paper is primarily limited to acceptance and performance testing (Part I of IEEE Std 115) and does not extend deeply into dynamic parameter determination. The lack of a unique quadrature-axis circuit (as with salient-pole rotors) simplifies much of the typical work. Discussion of test procedures for the more general case, including salient-pole rotors is not included here although this would be a worthy undertaking. In that vein, Miller[6], Klöckl [7] and Štumberger [8, 9] address the general case of PM machine parameter determination including non-saliency, but they do not relate their work to established standards. Slemon addresses both saliency and saturation in synchronous machine equivalent circuits with work spanning a few decades [10, 11].

Stator tests are generally unchanged between the conventional synchronous machine and the PM machine, this includes but is not limited to insulation resistance; dielectric and partial discharge; and winding resistance. Since there are no field windings only the armature windings are tested. Machine-level tests such as those used for shaft current and bearing insulation; telephone-influence-factor; acoustic noise; and waveform quality can be applied directly, however the definition of line-charging capacity excludes PM machines since the field excitation cannot be brought to zero (and line-charging capacity is not relevant for ASD connected machines in general).

Interpretation of short-circuit test data for high-speed PM machines will be different from a conventional WFSM. In particular, the transient reactance is undefined although not without a useful equivalency [12, 13] and the relative magnitudes of sub-transient reactance when comparing SMPM machines to WFSMs is quite different. The PM machine lacks a field winding on the rotor, the effective magnetic air-gap of a high-speed PM machine is significantly larger than a typical WFSM, and the eddy-current paths cannot be neglected (especially during faulted operation and transient conditions; also considering that the rotor is rarely laminated, magnets are monolithic at least to some degree and the containment sleeve may be conductive).

Open-circuit (no-load), and short-circuit tests can be performed similar to IEEE Std 115 however, only a single value of field excitation is possible with a PM machine. This simplifies the test procedure greatly, but has implications on the data available for each test. Whether obtained via separate-drive, electric-input or retardation methods, the “saturation curves” of the PM can only be obtained at a single point (Figure 1). The

line representing an equivalent field current of 1pu intersects the open circuit saturation curve (at point A) but does not intersect the zero PF rated current saturation curve (B), which is performed in an over-excited state. The short-circuit point, C, for a PM machine is more typical of that indicated in Figure 1 since for the rated equivalent-field-excitation the short-circuit current exceeds the rated current.

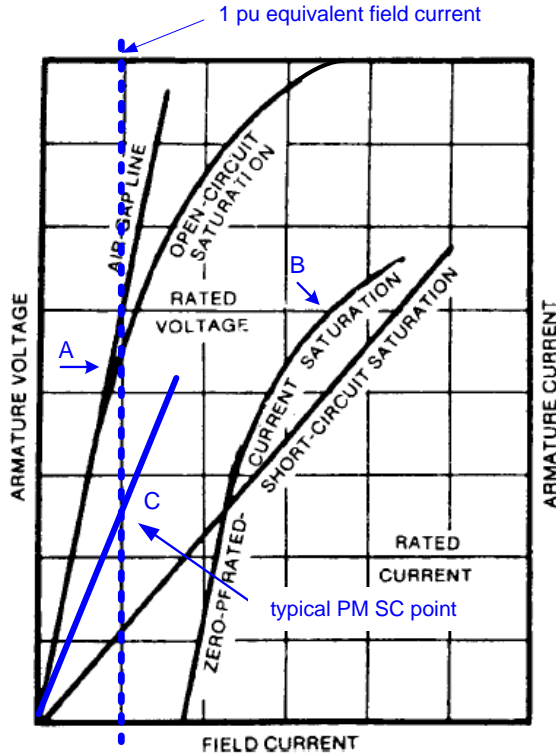


Fig 1. Curves from separated-drive method presented in [1].

Torque tests as described in IEEE 115 [1] are even more problematic since the field of the PM machine can be neither opened nor shorted as described. However, the general assumption is that PM motors will be coupled to an adjustable speed drive (ASD) and that (high frequency) PM generators will power a DC bus through an active power converter.

Section II of this paper discusses how test methods for WFSMs can be applied to PM machines. Section III explains how to interpret test results to further determine machine performance, in particular efficiency. Section IV reaffirms the importance of robustness to magnet demagnetization, while Section V highlights some mechanical considerations with special attention paid to rotor integrity.

II. APPLYING CONVENTIONAL TEST METHODS

A. Separate-drive method

IEEE 115 and API 546 [2] present a separate-drive test to segregate the losses and calculate the unsaturated inductance, X_{du} , of conventional synchronous machines. The WFSM excitation losses are either measured or computed directly and are not included in loss calculations in either open-circuit (OC)

or short-circuit (SC) loss calculations (there are no excitation losses for a PM machine). The machine under test (MUT) is driven at rated speed by a motor or dynamometer until the bearings of the MUT reach a stable temperature. The no-load losses of the driving motor should be known. The NL loss of the MUT is the power input to the driving motor minus the losses of the driving motor at that operating point. However, the loaded losses of the driving motor may not always be known – these may be small and in that case the NL loss of the MUT is approximated as the input power to the driving motor minus its NL loss. Also, a torque meter can be used between the driving motor and the MUT (Equation 1) and the results compared, however for large machines direct measurement of mechanical power is discouraged, IEEE Std 115 (Section 4.1.1) [1]. The losses of the MUT can be calculated from the measurement of speed and mechanical torque for these cases.

$$P_{in} = \omega \cdot T_m \quad (1)$$

The variable ω is the angular speed in rad/s and T_m is the mechanical torque in Nm. The open-circuit saturation curve (see Fig 1) can be obtained from the reading of terminal voltage (V_t) and excitation or field current (I_f) at rated speed [14].

The core loss of the MUT is segregated from the total no-load loss at any excitation repeating the no-load test with the field current set to zero. When I_f is zero, the mechanical input power of the MUT corresponds to the mechanical loss. At non-zero excitations the core loss is equal to the no-load loss minus the excitation loss and the mechanical losses (friction, windage, and bearing losses). The excitation loss is calculated from the known field winding resistance (at temperature) and the field current.

Although there are no ohmic excitation losses associated with a PM machine, since the excitation flux cannot be disabled, the core losses cannot be separated from the mechanical losses. However, if an identically sized, but un-magnetized rotor can be replaced in the MUT then the mechanical losses can be extracted and the core loss can be determined. In certain machine designs eddy-current loss during no-load cannot be neglected. For these machines the core loss computed from this method will include those eddy-current losses [3].

The short-circuit test can also be performed using the separate drive method. For this condition the MUT is run up to the rated speed with the armature short-circuited. The short-circuit characteristic is obtained for a WFSM from the range of armature and field currents, but for a PM machine the short-circuit characteristic is a single point corresponding to the equivalent field current and the armature current (which will be invariant with machine speed). The friction & windage loss, determined above, is subtracted from the input power to obtain the short-circuit loss. The stray-load loss is the difference between short-circuit loss and armature winding loss (calculated directly from the measured current and the DC resistance of the armature winding).

The unsaturated synchronous reactance for a WFSM can be obtained from the open-circuit saturation and the short-circuit saturation tests, as the ratio of the field current at base armature current (I_{FSI}), from the short-circuit test, to the field current at base voltage (I_{FG}) on the airgap line [1].

$$X_{du} = \frac{I_{FSI}}{I_{FG}} \quad [\text{p.u.}] \quad (2)$$

However this cannot be calculated in the same fashion for a PM machine. Instead, the open-circuit voltage is divided by the short-circuit current from point C to obtain the unsaturated impedance, or (after dividing by frequency in radians per second) the unsaturated direct-axis inductance in Equation 2. Point A of Figure 1 corresponds to the open-circuit voltage (V_{OC}) measured directly at the machine terminals. Point C represents the short-circuit current (I_{SC}).

$$L_{du} = \frac{V_{OC}}{2\pi \cdot f \cdot I_{SC}} \quad [\text{H}] \quad (2)$$

In (2) f is the electrical frequency in hertz. This “unsaturated” inductance obtained by this method will be slightly higher than a truly unsaturated inductance since there is no means to obtain the air-gap line for the PM machine with the open-circuit test. However this will be the minimum obtainable direct-axis inductance and is practically of as much use as a truly unsaturated value.

B. Electric-input method

The electric-input test for conventional WFSMs is described in IEEE Std 115 where the MUT is run as an unloaded synchronous motor. The total losses are measured from the electrical input terminals and include additional armature loss above the losses cited in the separate drive method. The total loss curve versus armature current (I_s) is extrapolated to $I_s = 0$ A to separate the no-load losses from the short-circuit losses. By subtracting this extrapolated value from the total loss at any armature current, the short-circuit loss is obtained for the corresponded armature current value. The stray-load losses are calculated from the short-circuit losses as in the separate drive method.

The open-circuit test procedure is unchanged between WFSM and a PM machine, but the “short-circuit” test using the electric-input method is quite different. The uncoupled PM machine makes use of an ASD with field-oriented control (FOC) to inject demagnetizing current into the MUT (although direct torque control or flux vector control algorithms could be employed as well), lowering the terminal voltage while increasing the current. This is closer to an under-excited zero-power factor (ZPF) test than a short circuit, but as the voltage is lowered and the current increased the short-circuit condition is approached.

For an ASD-driven PM machine, the q -axis current component (I_q) is established by the power needed to supply the losses. The angle of vector current (γ) of the d -axis current component (I_d) can be controlled and therefore, the magnitude of the input current can be increased up to the thermal limit (either ASD or MUT or both), approaching the expected short-circuit value. The input power corresponds to total losses of the machine under load (with the exception of the lower core losses experienced due to the lower terminal voltage) and can be directly measured or calculated from the input electrical parameters with the same caveats as with the conventional WFSM.

The measurement of current and voltage waveforms allows calculating the synchronous inductance. The power-per-phase is described by (Equation 3)

$$P_a = -\frac{1}{2} \frac{V_t \cdot V_{OC}}{X_d} \sin(\delta) \quad (3)$$

where δ is the load angle. The voltage relationship of phasors diagram shown in Fig 2 can written as,

$$V_t \angle 0^\circ = V_{OC} \angle \delta + jX_d I \angle \theta \quad (4)$$

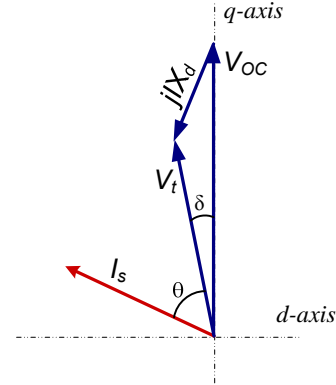


Fig 2. Phasor diagram for no-load motor operation

Equations (3) and (4) are used to develop a two-equation system with unknowns: δ and X_d . Since the frequency is known, the synchronous inductance value is straight forward and obtained with Equation 5

$$L_d = \frac{X_d}{2\pi \cdot f} \quad (5)$$

Although the ZPF testing can approximate the SC condition, it is not exact. Additional core loss is present as evidenced by the non-zero terminal voltage. Furthermore when efficiency calculations are required the core loss will be doubly counted if the NL loss is added to the SC loss to arrive at total losses as is the case for WFSMs. The ASD can be used to augment the data available to arrive at a better SC loss. The ZPF condition is repeated at multiple excitations and the measured loss is plotted versus resultant flux. The SC loss to be used in the efficiency calculation is then extrapolated from the zero resultant-flux intercept. This is analogous to some of the procedures given in IEEE Std 115.

C. Retardation Method

The retardation method relies on the relationship between the deceleration rate and total losses and can be applied directly whether WFSM or PM machine. The loss can be determined by the following equation (where ω is the rate of angular velocity of the rotor in rad/s and J is the moment of inertia of rotating parts, $\text{kg}\cdot\text{m}^2$):

$$Loss[W] = \omega \cdot J \cdot \frac{d\omega}{dt} \quad (6)$$

The losses obtained via the retardation method for the open-

circuit and the short-circuit test are the same as the losses obtained by the separate drive method. The preferred approach for PM machine testing using the retardation method is to run the machine up to speed in the same test configuration as with the electric-input method, but recording deceleration rate after either opening the ASD (OC test) or opening the drive and closing a shorting contactor (SC test).

D. Heat Transfer (Calorimetric) Method

This method is especially useful for machines with closed (or highly instrumented) cooling systems. It is based on the criteria that the heat produced is equal to the heat removed when in thermal steady-state. The application of this method is the same whether for a WFSM as discussed in IEEE Std 115 or for a PM machine. Machines may have multiple cooling medium (air, oil, water) and separate, dedicated circuits for individual portions of the machine. Each of these heat removal paths must be handled properly, and it may be necessary to restrict or re-direct flow during testing simply to obtain appropriate measurements of separate flow paths. For high-speed machines where bearing losses are not insignificant, the temperature and flow of the bearing lubrication circuit must be included in the heat removal calculations. The lubrication circuit may carry away losses in addition to those generated in the bearings, although significantly less likely in a PM machine than with other types of machines.

E. Loaded Generator Test.

Additional loaded generator tests can be carried out to obtain the synchronous inductance on PM machines. Using a resistive load bank, the angle between terminal voltage and the current is zero (unity PF) and the generator does not deliver reactive power.

$$Q_a = \frac{1}{2} \left[\frac{V_t^2}{X_d} - \frac{V_t \cdot V_{OC}}{X_d} \cos(\delta) \right] = 0 \quad (9)$$

For this particular condition the load angle can be calculated from (15) by,

$$\delta = \cos^{-1} \left(\frac{V_t}{V_{OC}} \right) \quad (10)$$

The synchronous reactance can be obtained from (3) as,

$$X_d = \frac{V_t \cdot V_{OC} \sin(\delta)}{2P_a} \quad (11)$$

The equation (5) can be used to calculate the synchronous inductance.

F. Torque Tests

Since the field of a PM machine can be neither open nor shorted, the torque tests prescribed in IEEE Std 115 cannot be applied directly. The speed-torque tests are generally

applicable for line-started machines, but a ASD driven PM machine will be influenced to a great degree by the ASD starting algorithm and the objective during starting for the particular application. The ability to control maximum torque (or to control torque within a pre-determined percentage) at overspeed is susceptible to the rotor position estimation and/or measurement method. If a locked-rotor test is to be undertaken, the scale and beam method is a preferred approach, however care must be taken in choosing a high bandwidth load cell and data-acquisition system as the "scale". The inductive, asynchronous torque may be quite low for large-gap PM machines relative to the rating, the starting philosophy instead relies on a robust control from the ASD. If a reliable indicator of starting performance is desired, then the ASD software (and hardware topology) should be reliably replicated if the appropriate model ASD is not available.

G. Temperature Tests

Temperature tests can be performed on a PM machine with ASD in accordance with Section 6.2.3 [1], the ZPF test method.

III. PERFORMANCE OF THE MACHINE

The performance of the MUT can be evaluated from the test results. The loss calculation determines the efficiency and the equivalent circuit parameters allow the estimation of the power conversion for any operating condition.

A. Simple Equivalent Circuits

The parameters measured or calculated from the tests allow construction of the simple per phase equivalent circuit, shown in Fig 5.

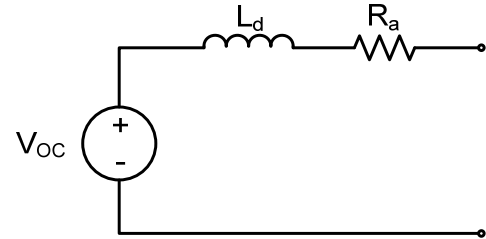


Fig 5. Simple per phase voltage-driven equivalent circuit

The stator per phase resistance (R_a) is typically the DC value measured at the machine terminals and corrected for the operation temperature of the winding but an additional AC effect can also be included. A value for R_a can be calculated by applying an AC voltage on the stator coil and measuring the resultant current at a stable temperature. From this method, R_a also includes the iron loss produced by the ac voltage in the stator core as well as any eddy-current losses, however as this is typically a small voltage the additional losses may not be significant. Also, if this test is performed on the stator alone, rather than as an assembled motor with the rotor inserted into the bore, the flux paths will be quite different (assuming three-phase AC voltage is applied to obtain a rotating field).

Slemon presents [10, 5] the current-driven equivalent circuit shown in Fig 6. The field excitation of the permanent magnets is

represented as constant current source. The synchronous inductance is split in two components (magnetizing and leakage),

$$L_d = L_{dL} + L_{ML} \quad (12)$$

Where L_{dL} represents the total stator leakage inductance produced by the flux on the slot, tooth top, zig-zag, harmonic and end-turns. The component L_{ML} is the magnetizing inductance in the airgap.

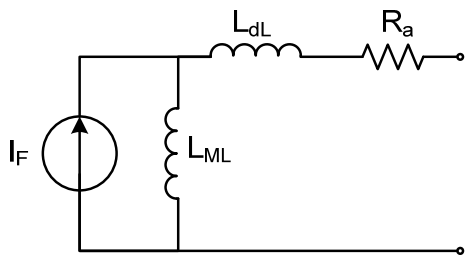


Fig 6. Simple per phase current-driven equivalent circuit

Core loss resistors can be added to the equivalent circuit (Figure 7), the values of which can be calculated from test data [10]. For high frequency machines it will likely be necessary to include these enhancements to properly account for the losses measured and when attempting to back-calculate the remaining equivalent circuit parameters. These core-loss resistors will vary with excitation frequency.

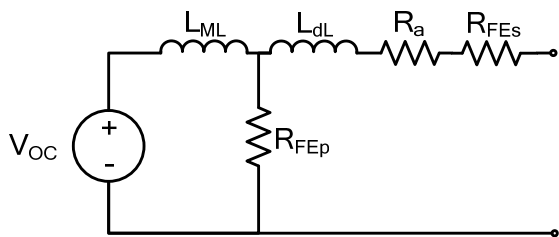


Fig 7. Enhanced per phase voltage-driven equivalent circuit including parallel, R_{FEP} , and series, R_{FEs} core loss resistors

The equivalent circuits of Figures 5-7 are suitable for PM machines at lightly saturated or unsaturated operating conditions. To properly account for saturation more detailed lumped-parameter (LP) models have been developed, however the preferred approach is to employ numerical techniques.

B. Numerical and Analytical Methods

Although both LP models and finite-element (FE) models have been employed to predict performance, FE models are preferred for highly saturated operating conditions, for detailed loss analysis and faulted operation [12, 8]. If a numerical or analytical method is used to support performance calculations, then the validation of that method should be agreed upon by manufacturer and purchaser. For determination of some quantities, the use of these methods cannot be avoided. Stator

core loss and eddy-current losses in monolithic conductors are the typical culprits.

The no-load loss, obtained by either measurement method can be segregated analytically [13] if an unmagnetized “dummy” rotor is not available for the separate-drive method. The windage loss can be calculated using the air gap dimensions and the temperature measured during no-load tests. The recorded supply and outlet temperatures and mass-flow rate of the coolant allows to estimate the bearing losses. The difference between no-load losses and windage and bearing loss results in the total magnetic losses. Fig 8 depicts the typical loss segregation for a PM machine using an analytical method.

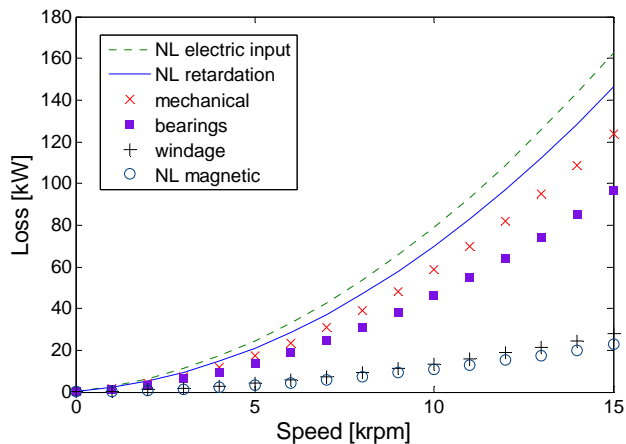


Fig 8. Typical no-load loss segregation: Analytical Method

The temperature distribution recorded during testing can be used by a thermal model to segregate the losses on liquid/air cooled PM machines [13]. The total losses measured are segregated in an attempt to reproduce the temperature distribution found during the test. The armature winding loss is split between the portion of winding in the slots and the end-turn winding. A heat balance from the measured flow and temperature of the cooling media and the prediction of the heat removed by convection should agree with the total loss measured by any method.

Alternatively, the mechanical losses may be separated from the NL losses by operating the machine at a few ZPF conditions and plotting the measured loss (minus the copper loss and electric drive induced harmonic losses, the far right column of Table I) versus terminal voltage. By extrapolating the curve down to zero voltage a reasonable approximation of the mechanical losses alone can be obtained.

C. Efficiency

The efficiency (η) of the PM machine should be calculated using the segregated-losses method using the total losses obtained from the methods outlined previously. An example is prepared in the following tables.

TABLE I
EXAMPLE DATA FOR ZPF TESTS

Phase Current [Arms]	Terminal Voltage [Vllrms]	ZPF loss [kW]	Copper Loss [kW]	Remaining Loss ¹ [kW]
890	2243	165.4	15.48	133.55
601	3219	160.2	7.05	136.84
400	3896	158.9	3.13	139.42
200	4573	159.7	0.78	142.58

TABLE II
EXAMPLE EFFICIENCY CALCULATION FOR RATED OPERATION: 8 MW, 15 krpm, 890 A

Value	Description
0.008 Ohms	Measured line-to-line resistance at 20 °C
0.0065 Ohms	Calculated line-to-neutral resistance at 180 °C
146.4 kW	² Measured NL OC loss at 15 krpm
162.74 kW	¹ Measured NL input power at 15 krpm
25.7 A	¹ Measured NL current
0.013 kW	Calculated NL stator winding loss, 180 °C
16.33 kW	Calculated loss due to ASD harmonics
123.6 kW	Extrapolated mechanical loss from Table I
165.4 kW	¹ Measured ZPF loss; 15 krpm, 890 A
7918 kW	Calculated shaft power; 15 krpm, 890 A
41.80 kW	Calculated SC loss = ZPF loss - mech. loss
188.20 kW	Calculated total loss = SC loss + NL OC loss
97.7 %	Calculated efficiency at rating = shaft output divided by (total loss + shaft output)

¹Electric input method ; ²Retardation method

The example makes only limited use of analytical models and instead is driven principally by ZPF and NL loss measurements. The rated input power can be a measured value if that data is available. The error in calculated efficiency for this particular example was found to be less than 0.1% which corresponds to roughly 3 kW of displaced loss.

IV. DEMAGNETIZATION ROBUSTNESS

Irreversible demagnetization occurs when the temperature and flux-density dependant operating point of the magnet extends below the linear portion of the B-H curve. Modern high megagauss-oersted (MGO) magnet materials are able to resist demagnetization in most applications because of linearity over wide range of the third quadrant of the B-H curve at the operating temperature. However, as MGO-ratings increase, temperature stability typically decreases. Careful attention must be paid to the specific magnetization curve of the magnet employed in each design, not only for normal operation, but also for faulted conditions and during the manufacturing process. In particular if the manufacturing includes heating of the magnets or if a rotor is planned to be stored at an elevated temperature outside of the stator, a flux shunt may need to be employed to prevent demagnetization, most usually noticeable at physical boundaries of magnets when flux focusing may occur.

For some machine designs, a three-phase short-circuit test can be performed without compromising the rotor magnets. The details of single tests, repeated and sustained faults must be jointly agreed upon by the manufacturer and purchaser for these cases especially if considered as part of acceptance rather than type testing since both rotor and stator damage is possible. As application requirements become more demanding and power density increases a particular PM machine may not survive a three-phase short circuit without some degree of demagnetization. Requirements in this regard must be clear between manufacturer and purchaser since is not necessarily explicitly required that a PM machine survive faulted operation with no loss of performance. Near short-circuit testing can still be performed by limiting the fault current to a predetermined acceptable-level.

A general test procedure to validate robustness to demagnetization is explained in [13] and further discussed here: first record the characteristic open-circuit voltage measurement, secondly perform the short-circuit test while limiting the current to safe levels, and finally repeat the open-circuit testing. There is a need to correct for magnet (and/or ambient) temperature, to this end the OC tests can be performed after a "cold soak" or at the beginning of work-day. During prolonged testing (especially during product development) it is often good practice to systematically perform OC tests at the beginning of each work-day so that the results can be quickly interpreted and flag unanticipated demagnetization from the previous days testing.

V. MECHANICAL CONSIDERATIONS

The most important differentiator between a conventional machine and a high-speed permanent-magnet machine is high-speed operation (beyond the rotor topology, although each rotor topology imposes specific feasibility constraints). After the rotor integrity at speed, the immediate concern for the mechanical components is placed on the bearings and couplings. Since other comparably sized turbo machinery exist which run at the higher speeds; bearing and dynamic response design and qualification limits have already been explored and set into standards, such as API 610 and 617 [15, 16]. The limits set down in these standards merely need to be applied to the high-speed permanent-magnet machine for acceptable long term operation and it is expected that will be so in the next revision of API 546 [17].

A solid steel shaft has a significant stiffness advantage over a laminated core construction and allows the rotor to obtain high speeds while operating below the bending modes. However the surface-mounted magnets need to be positively held to the rotor shaft throughout the operating speed range with some margin. Therefore, the primary consideration for rotor integrity which is unique to the high-speed permanent-magnet machine is magnet containment. This is a critical design aspect for safe machine operation at high speeds and can be accomplished in a number of ways. As discussed in [13] and [18] the ability of the permanent-magnet machine to go to high speeds is due to its rotor construction. The PM machine of Weeber [19] uses a conductive, high-strength "superalloy" others have chosen other high-strength metals [3, 20] such as inconel (probably the most common choice) or MP35N; the machine of Smith [4] uses retaining brackets; but many others have considered carbon-fiber composite sleeves of different types as the preferred method of magnet retention [21, 22, 23].

Inconel, as with most metallic sleeves, has advantages inherent to the manufacturing process. Since the manufacturing process is simple and repeatable the sleeve material properties are easy to predict and the behavior of the sleeve is consistent. An application specific advantage of the inconel sleeve is it being a good physical barrier between the magnets and any rotor gap fluid, especially suited to corrosive or abrasive environments. Major disadvantages of a metallic sleeves are the strength per unit weight compared to carbon fiber composite and the much higher conductivity, which will tend to increase eddy currents [3]. Also there are manufacturing challenges to be overcome with the shrink-fit a sleeve over a long, large diameter rotor (this limits the pre-stress that can be achieved which directly relates to magnet containment).

Carbon-fiber composites have very high strength in tension making them ideal for magnet containment, however they are not without manufacturing challenges. There are many different types and manufacturing processes for a composite sleeve: each manufacturer will likely have intellectual property related to design, analysis, and process control that is specific to their type of sleeve. Therefore consistent behavior of any composite magnet-retention sleeve should be demonstrated with statistical significance and included in any qualification or acceptance plan.

The magnet containment sleeve should be designed to prevent magnet lift-off, which happens when the contact pressure between the magnets and rotor hub reaches zero; and sleeve burst, which is when the hoop stress in the sleeve exceeds the tensile strength of the material. The operating points where these conditions must be satisfied need to be defined carefully in terms of temperature and speed. Limits for magnet lift-off and sleeve burst are contrary; increasing the margin on one decreases the margin on the other.

Verification of analytical tools is often accomplished through overspeed spin and burst testing (increasing the operating speed on a test sample until the magnet containment sleeve bursts). Burst testing by itself is informative and critical for confirming a predicted burst speed. However significant information can also be garnered from spin testing. A typical spin-test rig hangs the test sample vertically from an air turbine or other prime mover with some type of damping on the shaft. In this configuration the test sample spins about its own center, isolating the dynamic effects driven by just the shaft from the rest of the system.

The dynamics of the shaft monitored under different conditions will highlight the behavior of the shaft: for example to detect the proper function of the magnet-containment sleeve in terms of magnet lift-off, the rotor test sample can be cooled to the minimum application temperature and spun to full operating speed, numerous cold cycles may also be completed to add fidelity to the results. If the synchronous vibration of the shaft is increased from the room temperature operation spin then magnet lift-off is likely.

Regardless of material selection the magnet-containment sleeve is critical to safe operation of the machine and therefore must be held to tight design and qualification limits. The magnet-containment sleeve should prevent magnet lift-off and burst over the range of operating (and storage) temperatures and speeds. The sleeve-sizing analytical tools used in the design should be verified with hardware testing. Design rules should assign an appropriate margin between calculated performance and customer requirements, based on the fidelity

of the design tools used and the variation expected in the manufacturing process (especially including material properties).

VI. SUMMARY & CONCLUSION

There has been a recent impetus to include PM machines in IEEE standards, but this should not be limited to the relatively small line frequency machines investigated by Melfi [24]. Instead, large, high-speed PM machines need specific consideration, either in a new standard or in new revisions of existing standards (much in the same way that Rama's work [25] on ASDs heralded changes to API 541 [26] and in turn API 546 [17]). Beyond even what is presented here, salient-pole rotors, and more detailed equivalent circuits including saturable (cross coupled) inductances should be considered.

TABLE III
TEST METHODS AND COMPLICATIONS

Method	Complications
Separate drive	Driving machine losses must be well known or accurate torque meter must be available
Electric input	Measuring devices must be sized properly; phase angle errors due to sensor lag; VFD harmonics may significantly increase core and eddy-current losses; OC run at unity PF not MTA
Retardation	Need inertia of entire mechanical system; when using driver losses must be known; speed measured by tachometer, encoder, or voltage waveform
Calorimetric	Multiple coolants may be present; fluid/gas measurements often inaccurate or not resolved enough; heat lost to environment (radiation, conduction, convection) must be estimated

TABLE IV
SEGREGATION OF LOSSES OBTAINED BY TEST

Test	Method	Parameters	Losses
open circuit	separate drive	Voc	{1}
short circuit	separate drive	Isc	{2}
"open circuit"	electric input	Vt-Voc	armature + {1}
"zero power factor"	electric input	Xd	core + {2}
open circuit	retardation	Voc	{1}
short circuit	retardation	Isc	{2}
any	calorimetric		total loss

{1}: no-load (NL) losses: mechanical (friction & windage), core, eddy-current
 {2}: mechanical + short-circuit (SC) losses: armature, stray-load, eddy-current

Separate drive and retardation methods are preferred for parameter determination and should be used when possible. The electric-input method is required to capture the impact of drive harmonics on loss measurements. Manufacturers should

expect to apply all methods (especially during type-testing), but end-users should specify their preferred acceptance test method which will likely be influenced by the machine installation.

PM machines have many features in common with conventionally deployed machines, in particular the stator construction, bearing system, and housing construction. However rotor demagnetization robustness and magnet containment require special consideration in design qualification and risk mitigation. Although the rotor field is not adjustable, a viable means for determining efficiency has been presented and equivalent circuit parameter can be determined using only the types of tests already familiar to users of large synchronous machines.

VII. ACKNOWLEDGEMENTS

The authors would like to extend their gratitude to the reviewers who contributed to the completeness of this paper and to Tony Li for working through the example calculations.

VIII. REFERENCES

- [1] IEEE Std 115-1995, *IEEE Guide: Test Procedures for Synchronous Machines*, IEEE Std., December 1995.
- [2] API Std 546-1997, *Brushless Synchronous Machines - 500 kVA and Larger*, API Std., June 1997.
- [3] D. M. Saban, "Eddy current losses in the sleeves of high-speed synchronous machines," PhD Thesis, University of Wisconsin - Madison, 2006.
- [4] J. S. Smith and A. P. Watson, "Design, manufacture, and testing of a high speed 10 mw permanent magnet motor and discussion of potential applications," in *Proceedings of the 35th Turbomachinery Symposium*, 2006, pp. 19–24.
- [5] G. R. Slemon, *Electric Machines and Drives*. Addison-Wesley, 1992.
- [6] T. J. E. Miller, "Methods for testing permanent magnet polyphase ac motors," in *IEEE Proceedings of the Industrial Applications Society*, 1981, pp. 494–498.
- [7] B. Klöckl, "Measurement based parameter determination of permanent magnet synchronous machines," Master's thesis, Graz University of Technology, 2001.
- [8] B. Stumberger and B. Hribernik, "Calculation of two axis parameters of synchronous motor with permanent magnets using finite elements," *Electric Machines and Drives*, pp. 98–100, May 1999.
- [9] B. Stumberger, B. Kreca, and B. Hribernik, "Determination of parameters of synchronous motor with permanent magnets from measurement of load conditions," *IEEE Transactions on Energy Conversion*, vol. 36, no. 4, pp. 1413–1416, December 1999.
- [10] G. R. Slemon, "Analytical models for saturated synchronous machines," in *IEEE Transactions on Power Apparatus and Systems*, no. 2, March 1971, pp. 409–417.
- [11] —, "An equivalent circuit approach to analysis of synchronous machine with saliency and saturation," *IEEE Transactions on Energy Conversion*, vol. 5, no. 3, pp. 538–545, September 1990.
- [12] K. W. Klontz, T. J. E. Miller, M. I. McGilp, H. Karmaker, and P. Zhong, "Short-circuit analysis of permanent-magnet generators," in *Proceedings of the International Electric Machinery Development Conference (IEMDC)*, in press, 2009.
- [13] D. M. Saban, C. Bailey, D. Gonzalez-Lopez, and L. Luca, "Experimental evaluation of a high-speed permanent-magnet machine," in *Proc. 55th IEEE Petroleum and Chemical Industry Technical Conference PCIC 2008*, 22–24 Sept. 2008, pp. 1–9.
- [14] A. E. Fitzgerald, C. Kingsley Jr., and S. D. Umans, *Electric Machinery*, 6th ed. McGraw Hill, 2003.
- [15] API Std 610-2004, *Centrifugal Pumps for Petroleum, Petrochemical and Natural Gas Industries, Tenth Edition*, API Std., October 2004.
- [16] API Std 617-2002, *Axial and Centrifugal Compressors and Expander-compressors for Petroleum, Chemical and Gas Industry Services, Seventh Edition*, API Std., July 2002.
- [17] B. Lockley, M. Chisholm, T. Griffith, G. D'Alleva, and B. Wood, "API 546 3rd edition - making synchronous machines better," in *Proc. 55th IEEE Petroleum and Chemical Industry Technical Conference PCIC 2008*, 22–24 Sept. 2008, pp. 1–8.
- [18] C. Bailey, D. M. Saban, and P. Guedes-Pinto, "Design of high-speed, direct-connected, permanent-magnet motors and generators for the petrochemical industry," in *Proc. IEEE Petroleum and Chemical Industry Technical Conference PCIC '07*, 17–19 Sept. 2007, pp. 1–5.
- [19] K. Weeber, C. Stephens, J. Vandam, J. Yagielski, A. Gravame, and D. Messervey, "High-speed permanent-magnet motors for the oil & gas industry," in *Proceedings of GT2007; ASME Turbo Expo 2007: Power for Land, Sea and Air*, 14–17 May 2007, manual entry.
- [20] N. Bianchi, S. Bolognani, and F. Luise, "Potentials and limits of high-speed pm motors," vol. 40, no. 6, pp. 1570–1578, Nov.–Dec. 2004.
- [21] A. Nelson, M. Baker, C. Huynh, L. Hawkins, and A. Filatov, "New developments in high-speed, direct-connected, permanent magnet motors and generators for marine applications," in *WMTC Conference Record*, 2006.
- [22] P. Beer, J. E. Tessaro, B. Eckels, and P. Gaberson, "High-speed motor designs for gas compressor applications," in *Proceedings of the Thirty-Fifth Turbomachinery Symposium*, 2006.
- [23] A. Binder, "Analytical calculations of eddy-current losses in massive rotor parts of high speed permanent magnet machines," *SPEEDAM 2000 ISCHIA*, pp. C2–1–C2–6, June 2000.
- [24] M. J. Melfi, S. D. Rogers, S. Evon, and B. Martin, "Permanent magnet motors for energy savings in industrial applications," in *Proc. Industry Applications Society 53rd Annual Petroleum and Chemical Industry Conference*, Sept. 11 2006–Oct. 15 2006, pp. 1–8.
- [25] J. C. Rama, "Supplemental guidelines for use with API Standard 541 when specifying motors for use with adjustable speed drives," in *Proc. IEEE Petroleum and Chemical Industry Technical Conference PCIC '93*, 1993, pp. 81–88.
- [26] API Std 541-2004, *Form-wound Squirrel-Cage Induction Motors- 500 Horsepower and Larger*, API Std., Rev. 4th, June.

IX. VITA

Dan Saban earned a BSEE degree from the University of Illinois - Urbana in 1992, a MSEE degree from Purdue

University - West Lafayette in 1993 and a PhD degree in Electrical Engineering from the University of Wisconsin - Madison in 2006 where he specialized in electric motor analysis. Additionally, he holds an MSEE (2002) and a MSME (2003) from University of Wisconsin - Madison with focuses on power electronics and controls, respectively. He is currently the Director of Technology for Direct Drive Systems and was previously employed by Hamilton Sundstrand and General Electric (concurrent with his advanced degrees). Throughout his 17 year career he has been involved in advanced electromagnetic design of electric machinery including new lamination and winding designs, design tools, and both prototype and product family development for commercial, industrial and aerospace applications. Dr. Saban is a senior member of IEEE and a registered professional engineer in Indiana and Illinois.

Cassandra Bailey was graduated in 2003 from Northwestern University with a Bachelors of Science degree in Mechanical Engineering and is a member of ASME and IEEE. She started as an Integrated Drive Generator Design Engineer with Hamilton Sundstrand designing an integrated variable speed transmissions and AC generators for various military aircraft applications. Currently, she is with Direct Drive Systems as a Project Engineer designing high-speed medium-voltage permanent-magnet machines.

Klaus Brun is presently the Manager of the Rotating Machinery Section at Southwest Research Institute in San Antonio, Texas. Dr. Brun received his PhD and Masters of Science degrees in Mechanical and Aerospace Engineering from the University of Virginia and a Bachelor of Science degree in Aerospace Engineering from the University of Florida. He is a member of the International Gas Turbine Institute Board of Directors, the past chair of the ASME-IGTI Oil & Gas Applications Committee, and a member of the Gas Turbine Users Symposium Advisory Committee. He is the inventor of the Single Wheel Radial Flow Gas Turbine.

Delvis Gonzalez-Lopez received the Electrical Engineer degree in 1997 and the Master in Science degree in 2001, from Central University of Las Villas, Cuba. He earned a Doctor in Engineering Science/Electrical Engineering degree in 2006 from the University of Concepcion, Chile. Currently, he is an Electrical Engineer for Direct Drive Systems. Dr. Gonzalez is an IEEE Member and his interests include design, optimization and control of electrical (primarily permanent-magnet) machines, magnetic bearings, and magnetic couplers.